The ROS-Mitophagy Signalling Pathway regulates liver endothelial cell survival during ischaemia-reperfusion injury

Bhogal, Ricky; Weston, Christopher; Velduis, Susanne; Henri GD, Leuvenink; Reynolds, Gary; Davies, Scott; Luu, Nguyet -Thin; Alfaifi, Mohammed; Shepherd, Emma; Boteon, Yuri; Wallace, Lorraine; Oo, Ye Htun; Adams, David; Mirza, Darius F; Mergentel, H; Muirhead, Gillian; Stephenson, Barnaby; Afford, Simon

DOI:
10.1002/lt.25313

PROF. DAVID H ADAMS (Orcid ID : 0000-0001-6776-0336)

DR. HYNEK MERGENTAL (Orcid ID : 0000-0001-5480-9380)

Article type : Original Articles

Title: The ROS-Mitophagy Signalling Pathway Regulates Liver Endothelial Cell Survival during Ischaemia-Reperfusion Injury

Ricky H. Bhogal[1,2], Christopher J. Weston[1], Susanne Velduis[3], Henri G.D. Leuvenink[3], Gary M. Reynolds[1], Scott Davies[1], Luu Nyguet-Thin[1], Mohammed Alfaifi[1], Emma Shepard[1], Yuri Boteon[1], Lorraine Wallace[1], Ye Oo[1], David H. Adams[1], Darius F. Mirza[1,2], Hynek Mergental[1,2], Gillian Muirhead[1], Barnaby F. Stephenson[1], Simon C. Afford[1]

[1]Centre for Liver Research, School of Infection and Immunity, Institute for Biomedical Research, The Medical School, Edgbaston, Birmingham, West Midlands. B15 2TT. United Kingdom.

[2]The Liver Unit, University Hospitals of Birmingham, New Queen Elizabeth Hospital Birmingham, Mindelsohn Way, Edgbaston, Birmingham. B15 2GW. United Kingdom

[3]University Medical Centre Groningen, University of Groningen, The Netherlands.

Corresponding Author:

Mr Ricky Harminder Bhogal PhD FRCS

Centre for Liver Research

School of Infection and Immunity

Institute for Biomedical Research

The Medical School

Edgbaston

Birmingham

West Midlands

B15 2TT. United Kingdom

E-mail: balsin@hotmail.com

This article has been accepted for publication and undergone full peer review but has not been through the copyediting, typesetting, pagination and proofreading process, which may lead to differences between this version and the Version of Record. Please cite this article as doi: 10.1002/lt.25313

Running Title: Autophagy Regulates Liver Endothelial Cell Survival during IRI

RHB, CJW, SV, SD LNT, MA, ES, LW, BS all performed experiments within the manuscript. RHB wrote the manuscript. DFM, HM, YO, SCA critical appraised the manuscript.

Conflict of Interests: The authors have no conflict of interests to declare.

Abbreviations: 7-AAD, 7-amino-actinomycin D; ATG, autophagy regulated proteins; LEC, liver endothelial cells; ROS, reactive oxygen species

Abstract

Background: Ischaemia-reperfusion injury (IRI) is the main cause of complications following liver transplantation. Reactive oxygen species (ROS) were thought to be the main regulators of IRI. However recent studies demonstrate that ROS activates the cytoprotective mechanism of autophagy promoting cell survival. Liver IRI initially damages the liver endothelial cells (LEC) but whether ROS-autophagy promotes cell survival in LEC during IRI is not known.

Methods: Primary human LEC were isolated from human liver tissue and exposed to an *in vitro* model of IRI to assess the role of autophagy in LEC. The role of autophagy during liver IRI *in vivo* was assessed using a murine model of partial liver IRI.

Results: During IRI ROS specifically activate ATG7 promoting autophagic flux and the formation of LC3B positive puncta around mitochondria in primary human LEC. Inhibition of ROS reduces autophagic flux in LEC during IRI inducing necrosis. In addition siRNA knockdown of ATG7 sensitized LEC to necrosis during IRI. *In vivo* murine livers in uninjured liver lobes demonstrate autophagy within LEC that is reduced following IRI with concomitant reduction in autophagic flux and increased cell death.

Conclusion: These findings demonstrate that during liver IRI ROS-dependent autophagy promotes LEC survival and therapeutic targeting of this signaling pathway may reduce liver IRI following transplantation.

Key words: Autophagy; Free radicals; Ischaemic liver injury; Necrosis

Introduction

The incidence of end-stage liver disease or cirrhosis continues to rise worldwide (1). The only curative treatment for liver cirrhosis remains transplantation. As part of liver transplantation the hepatic blood flow is temporary interrupted to aid surgery but this leads to the development of the ischaemia-reperfusion injury (IRI) once blood flow to the liver is restored (2,3). Moreover 20% of the complications following liver transplantation, including graft dysfunction and/or primary graft non-function, are directly attributable to IRI (4).

IRI is a pro-inflammatory antigen-independent process that causes liver parenchymal cell injury (4). Specifically, the first cell type to be injured by liver IRI are the liver endothelial cells (LEC) (5). However the mechanisms that regulate LEC injury during IRI remain to be fully determined. It is known that reactive oxygen species (ROS) are key regulators of liver IRI (2,6). ROS can be generated by both parenchymal and non-parenchymal cells (e.g. Kupffer cells) within the liver during IRI (6,7). Recent studies suggest ROS generated within liver parenchymal cells, such as LEC, may be integral to the development of liver IRI (6). Importantly ROS can have divergent effects upon cell survival with emerging evidence suggesting that ROS generation during early IRI is cytoprotective through its activation of the autophagy-signaling pathway (8,9).

Autophagy is an evolutionarily conserved process that is regulated by a distinct cellular machinery known as the autophagy related proteins (ATGs). Activation of autophagy allows cells to enclose targeted cargo in a double membrane structure known as an autophagosome during periods of cellular stress such as IRI (10). Following sequential maturation steps that involve various ATGs, ATG8/LC3B and the docking protein p62 regulate the fusion of the autophagosome with lysosomes to form autophagolysomes with resultant cargo degradation (11). The substrates from cargo breakdown are then available for anabolic cellular processes (10). Recently it has become apparent that the cargo targeted by autophagy can be highly selective leading to the elimination of mitochondria (mitophagy), endoplasmic reticulum (ERphagy) and bacteria (xenophagy) (10). In particular autophagy in LEC has recently been shown to be regulated by KLF2 (12). These studies suggest that failure of this mechanism of autophagy activation can lead to endothelial cell death during periods of stress and is associated microvascular dysfunction, a key feature of liver IRI (12).

There is growing interest in the regulation of liver IRI by autophagy (9) particularly because ROS has been shown to regulate the autophagy-signaling pathway (13). However the role of both ROS and autophagy in LEC remains to be determined although studies in cells of endothelial lineage such as Human Umbilical Vein Endothelial Cell and vascular endothelium suggest that autophagy is cytoprotective during oxidative stress (14,15). Our study investigated the role of ROS and autophagy in determining primary human LEC function during IRI.

Methods and Materials

LEC Isolation and Culture

Liver tissue was obtained via the Hepatobiliary and Liver Transplant Surgery program at the Queen Elizabeth Hospital Birmingham, UK, from fully consenting adult patients undergoing transplantation, hepatic resection for liver metastasis, hepatic resection for benign liver disease or normal donor tissue surplus to surgical requirements. Ethical approval for the study was grant by the Local Research Ethics Committee (LREC) (reference number 06/Q702/61). LEC were isolated from human liver tissue as previously described (16). Briefly, parenchymal cells were collected after collagenase digestion of mechanically disaggregated liver and were further purified by density gradient centrifugation over Percoll. Endothelial cells were isolated from the resultant heterogeneous cell mixture by positive immunomagnetic selection using antibodies raised against CD31 (Dako) and magnetic beads (Dynal) conjugated with goat anti-mouse antibody according to the manufacturer's protocol. All endothelial cells were maintained in complete media comprising Human Endothelial-SFM basal growth medium (Invitrogen) containing 104 U/ml penicillin and 10 µl/ml streptomycin, 10 ng/ml epidermal growth factor (R&D Systems), 10 ng/ml vascular endothelial growth factor and 10% heat-inactivated human serum (TCS Biologicals). All endothelial cells were plated out into collagen-coated culture flasks (Sigma) and maintained at 37°C in a humidified 5% CO_2 incubator until confluent. The endothelial cells were used for experiments only up to *passage 6*, and phenotypic identity and purity were confirmed by staining for endothelial markers as previously described (16). This rigorous standardized protocol used to isolate primary human LEC is well accepted and has been shown to maintain LEC function and phenotype and has been in longstanding use in our laboratory (17).

In vitro model of IRI

In experiments, primary human LEC were cultured in the conditions described above. LEC were used an in an *in vitro* model of IRI that we have previously described (6, 8, 18). Hypoxia was achieved by placing cells in an airtight incubator (Don Whitley) flushed with 5% CO_2 and 95% N_2 until oxygen content in the chamber reached 0.1%, as verified by a dissolved oxygen monitor (DOH-247-KIT, Omega Engineering, UK). Normoxia denotes LEC maintained in ambient oxygen conditions, hypoxia denotes LEC maintained at 0.1% oxygen for 24 hours and hypoxia-reoxygenation (H-R) denotes LEC kept at 0.1% oxygen for 24 hours and then transferred to ambient oxygen conditions for a further 24 hours. In experiments involving N-acetylcysteine (NAC) the antioxidant was made fresh as a stock solution and added using the correct dilution factor to the relevant experimental wells. Vehicle only wells were used as controls. NAC was added to LEC at the time of placement of cells into normoxia, hypoxia or H-R.

Determination of LEC ROS production, apoptosis and necrosis

Primary human LEC ROS production, apoptosis and necrosis during *in vitro* IRI was determined by using a three-colour reporter assay system that we have previously described (6). Briefly, ROS accumulation was determined using the fluorescent probe 2′,7′-dichlorofluorescin-diacetate (DCF) (Merck, 287810). Apoptosis was determined by labeling cells with Annexin-V (Molecular Probes, Invitrogen, A35122) and 7-Amino-Actinomycin D (7-AAD) (Molecular Probes, Invitrogen, A1310)

was used to assess necrosis. For flow cytometry at least 20,000 events were recorded within the gated region of the flow cytometer for each primary human LEC preparation in each experimental condition. Only the cells within the gated region were used to calculate Mean Fluorescence Intensity (MFI).

Transfection of ATG7 small interfering RNA (siRNA) in Primary Human LEC

Scrambled siRNAs and specific validated siRNAs for ATG7 were purchased from ThermoFisher Scientific. Primary human LEC were seeded in the wells of culture dishes. After 24 h, the cells were transfected with 50 nmol/L scrambled siRNAs or 50 nmol/L ATG7 siRNA using the Lipofectamine RNAiMAX transfection reagent (Invitrogen, Carlsbad, CA, USA) according to the manufacturer's protocol. Knockdown of ATG7 was confirmed with PCR using standard primers.

Immunofluorescence for LC3B Puncta and Dual Immunofluorescence for LC3B and Mitochondrial Marker TOMM-20 in Primary Human LEC

Following experiments primary human LEC were fixed in ice-cold methanol followed by serial washing with PBS. LEC were permeabilization in 0.1% Triton X-100 for 20 min at room temperature. LEC were then incubated in blocking buffer for 45 min. Cells were then incubated in primary rabbit anti-human LC3B antibodies (1:400, Cell Signalling Technology) or control antibody for 2 hour at room temperature. After rinsing with PBS, LEC were incubated with donkey-anti-rabbit IgG Alexa Fluor 594 secondary antibody (1:2000; Molecular Probes) for 1 h at room temperature. Cells were mounted with ProLong® Gold antifade with DAPI (Molecular Probes). Images were captured with a CCD camera and imported into Adobe Photoshop and LC3B puncta in cells was quantified using imageJ software.

For dual immunofluorescence experiments following incubation with IgG Alexa Fluor 594 secondary antibody, LEC were washed with PBS and incubated at room temperature for 1 hour with mouse anti-human TOMM20 antibodies (1:200, Abcam). After rinsing with PBS, sections were incubated with goat anti-mouse IgG Alexa Fluor 488 secondary antibody (1:1000; Molecular Probes) for 1 h at room temperature. Cells were mounted with ProLong® Gold antifade with DAPI (Molecular Probes). Images were captured with a CCD camera and imported into Adobe Photoshop. LC3B puncta and TOMM20 staining in cells were quantified using imageJ software.

Western blotting

For western immunoblotting studies, primary human LEC were lysed at the end of the relevant experimental period using NP-40 lysis buffer (20 mM TRIS-HCl pH 8 (Sigma-Aldrich, T3253), 137 mM NaCl (Sigma-Aldrich, S3014), 10% glycerol (Sigma-Aldrich, G5516), 1% Nonidet P40 (Sigma-Aldrich, 18896), 2 mM EDTA (Sigma-Aldrich, E6758). Protein concentration was determined by Bradford protein assay and 25 μg of protein was resolved on a 10% SDS-PAGE gel and transferred to a nitrocellulose membrane (Hybond; Amersham Biosciences, RPN3032D). The blotted membrane was blocked for 1 h at room temperature in TBS pH 7.4/Tween 0.1% (Sigma-Aldrich, P9416) containing 5% (wt/vol) bovine serum albumin (BSA) (Sigma-Aldrich, A9418). All primary antibody incubations were performed at overnight at 4°C in TBS-Tween 0.1% containing 5% BSA (wt/vol).

The incubation steps were followed by three washing steps of 5 min with TBS containing 0.1% Tween. All primary antibodies were purchased from New England Biolabs and used at a dilution of 1:1000 as per manufacturer's instructions. Specific primary antibodies used for primary human LSEC included: (1) BECN1 (3495), (2) LC3B (3868), (3) ATG5 (8540) and (4) ATG7 (2631) (5) p62 (5114). Binding of specific mAb was detected with a horseradish peroxidase-conjugated anti-rabbit IgG at a dilution of 1:2000 for 1 h (Sigma-Aldrich, A8792). Primary antibodies used for mouse liver lysates included: (1) ATG7 (8558) (2) LC3B (3868) (3) p62 (5114). Protein bands were visualized using the enhanced chemiluminescence detection system (Amersham Biosciences, RPN2109) followed by exposure of the membranes to Hyperfilm-ECL (Amersham Biosciences, 28-9068-37). Equality of protein loading on was checked by immunoblotting for β-actin (Sigma-Aldrich, A2228) (dilution 1:20000). All Western immunoblots were performed at least three times. Protein levels were quantified using densitometric scanning and normalized to loading control levels. Some samples required prolonged exposure of immunoblots for up to 48 hours at -4^{o}C.

In vivo model of Partial Liver Ischaemia-Reperfusion Injury

All animal experiments were performed at University Medical Centre Groningen (UMCG) in compliance with the guidelines of the local animal ethics committee according to Experiments on Animals Act (1996) issued by the Ministry of Public Health, Welfare and Sports of The Netherlands. Wild-type C57 Black 6 (C57/B6) mice were anesthetized with isofluorane inhalation. Following laparotomy an atraumatic clip was placed across the portal vein, hepatic artery, and bile duct just above the branching to the right lateral lobe. The median and left lateral lobes (approximately 70% of the murine liver mass) rapidly showed significant blanching. Following satisfactory clamp placement, the intestines were placed back into the abdominal cavity carefully and covered the incision with well-moistened gauze with saline. The ischaemic time used for the experiments was 90 minutes and reperfusion time was 6 hours. The animals were then placed into heated chambers were free access to chow and free water. Sham operated animals were handled in exactly the same manner other than undergoing clamping of the portal triad. Immediately following the reperfusion period animals were again anaesthesia with isofluorane. The laparotomy wound was opened and 10 µl of heparinised saline was injected directly into the IVC and then venous blood collected into a microsyringe. The animal was then euthanized by exsanguination. The liver was then removed.

Serum Preparation, Quantification of Liver Transaminase Levels

Serum levels of alanine aminotransferase (ALT) and aspartate aminotransferase (AST) was were quantitative indices of liver damage used to assess liver injury and could be quantified in serum obtained from mice subjected to liver IRI. The samples were processed and quantified at the UMCG clinical chemistry laboratory using standard operating protocols. Data are presented as units per litre (U/L) at 37°C.

TUNEL Assay

TUNEL assay was performed on mouse liver sections according to the manufacturer's instructions (Roche). Samples were air-dried for 30 minutes at RT and washed three times with PBS for 3 minutes each. The sections were pre-fixed with 1 % PFA for 10 minutes at RT, and then post-fixed by pre-

cooled ethanol/acetic acid (2:1) at -20°C for 5 minutes. The fixed tissue sections were incubated with DAPI for nuclei staining following exposure to equilibration buffer for 10 seconds at RT and TdT enzymes for 30 minutes at 37 °C. Images were captured with a CCD camera and imported into Adobe Photoshop. The quantification of TUNEL-positive LEC was performed by manually counting the number of TUNEL-LEC cells per randomly selected 10 high power fields (HPF) per section in a blinded fashion by GMR.

Histopathology, Immunohistochemistry and Immunofluorescence

Following exsanguinations, representative pieces of ischaemic or non-injured liver lobes were quickly removed and fixed in ice cold 10% phosphate-buffered formalin for 24 hours at 4°C. The tissue is then partially dehydrated with ethanol and embedded in JB4 plastic mounting media using standard histological methods. Five-micrometer sections cut and stained with haematoxylin and eosin (H&E). Immunoperoxidase staining for LC3B (rabbit monoclonal antibody, clone 5F10, New England Biolabs) and CD31 (goat polyclonal antibody, R&D Systems) were performed on the FFPE mouse liver tissue. Tissue sections were deparaffinized followed by antigen-retrieval. Antibodies were incubated at room temperature for 1 h at LCB (1∶ 400 dilution) and CD31 (1:100 dilution). Antibody staining was developed using the IMMPACT DAB detection system (Ventana Medical Systems) and accompanied by hematoxylin counterstain. Immunohistochemical staining was determined by quantifying total area stained per randomly selected 10 HPF per section using imageJ software.

For dual immunofluorescence tissue sections were deparffinized followed by antigen-retrieval. After washing in TBS-Tween0.1% sections were incubated with LC3B antibody (1:400) for 1 hour at room temperature followed by incubation with IgG Alexa Fluor 594 donkey anti-human secondary antibody. Sections were washed with TBS-Tween0.1% and incubated at room temperature for 1 hour with mouse anti-human CD31 antibodies (1:100, Abcam). After rinsing with PBS, sections were incubated with goat anti-human IgG Alexa Fluor 488 secondary antibody (1:2000; Molecular Probes) for 1 h at room temperature. Sections were mounted with Anti-Fade mountant (Molecular Probes) and images were captured with a CCD camera and imported into Adobe Photoshop. Immunofluorescence staining was determined by quantifying staining intensity relative to control using imageJ software.

Statistical Analysis

All data are expressed as mean ± SEM. Statistical comparisons between groups were analysed by Student's *t* test. All differences were considered statistically significant at a value of $p<0.05$.

Results

Human LEC Maintain Intracellular ROS throughout IRI that is inhibited by the General Antioxidant NAC

Isolated primary human LEC were exposed to our established *in vitro* model of IRI (6,8) and intracellular ROS assessed using DCF as described above. During normoxia LEC demonstrate high ROS content and exposure to hypoxia and then H-R does not significantly alter intracellular ROS content (Fig 1). Furthermore primary human LEC isolated from different liver diseases such as alcoholic liver disease, biliary cirrhosis and steatotic liver disease show similar intracellular ROS profiles during *in vitro* IRI (data not shown).

The general antioxidant NAC is able to efficiently inhibited ROS production within cells generated from a variety of sources including the mitochondria and cystolic enzymes (6). Incubation of primary human LEC with NAC significantly reduces intracellular ROS content during normoxia, hypoxia and H-R with maximal effects noted with 6 hours of NAC treatment in each experimental condition (Fig 2). Taken together these data demonstrate that primary human LEC maintain high intracellular ROS levels during *in vitro* IRI that can be inhibited by NAC.

Intracellular ROS Regulates ATG7 Activity, Autophagic Flux and LC3B Positive Puncta in Primary Human LEC during IRI

ROS has been previously linked to autophagy activation (13) and in primary human LEC NAC mediated ROS inhibition led to a specific reduction in ATG7 activity during *in vitro* IRI during normoxia, hypoxia and H-R (Fig 3) with no effect noted on ATG5, Beclin-1 or ATG 12 (data not shown). In the canonical autophagy signaling pathway ATG7 activation is upstream LC3B lipidation and autophagosome formation (10). The formation of autophagosomes can be investigated by assessing the ratio of LC3B:p62 deriving an assessment of autophagic flux. NAC reduced autophagic flux during *in vitro* IRI as demonstrated by the reduction in LC3B protein and increase in p62 protein during normoxia, hypoxia and H-R (Fig 3). These findings suggest that ROS specifically regulates ATG7 activity in human LEC during IRI the inhibition of which leads to a reduction in autophagic flux in primary human LEC.

To further assess autophagy flux in human LEC we used specific siRNA knockdown of ATG7 in LEC. As demonstrated in Fig 4(i) and 4(ii) this experimental approach decreased ATG7 expression by approximately 60% in primary human LEC. Moreover ATG7 knockdown inhibits autophagic flux as demonstrated by the decrease in LC3B and accumulation of p62 in human LEC during normoxia, hypoxia and H-R (Fig 4(ii). The inhibition of ATG7 activity in primary human LEC sensitizes cells to necrosis and not apoptosis (data not shown) during normoxia, hypoxia and H-R (Fig 4(iii) suggesting that ATG7 function is integral to LEC survival during IRI.

ROS-dependent ATG7 activation also affects tempro-spatial LC3B positive puncta in LEC during IRI as demonstrated by the loss of LC3B positive puncta throughout the cytoplasm after NAC treatment (Fig 5). Importantly this phenomenon was noted in normoxia, hypoxia and H-R. Taken together these findings shown that ROS-dependent ATG7 activity mediates autophagic flux and autophagosome formation in primary human LEC during IRI.

ROS Mediate Mitophagy in Human LEC during IRI

Recent studies have suggested that selective forms of autophagy occur within specific disease processes (10). It is well established that during liver IRI dysfunctional mitochondria contribute to parenchymal cell injury (19). Indeed the selective elimination of dysfunctional mitochondria, known as mitophagy, has recently been linked to progression of liver IRI (9). We assessed whether LC3B positive puncta are found in proximity to mitochondria in primary human LEC during IRI. To investigate this we utilized the specific mitochondrial marker TOMM-20. Indeed TOMM-20 and LC3B co-localise within human LEC during IRI (Fig 6). Importantly inhibition of ROS with NAC for 6 hours caused a significant reduction in TOMM-20 and LC3B dual positivity suggesting that ROS-dependent ATG7 is a key regulator of mitophagy in primary human LEC during IRI.

ROS Inhibition Sensitises Human LEC to Necrosis during IRI

The above data demonstrate that ROS activates autophagy/mitophagy in primary human LEC and therefore is would be expected that inhibition of ROS would induce cell death if autophagy/mitophagy were a cytoprotective mechanism in LEC as suggested in Figure 4 with ATG7 knockdown sensitising LEC to necrosis. Accordingly we found NAC-mediated ROS-ATG7 inhibition increased human LEC necrosis during IRI (Fig 7). Maximal effects were noted during H-R after 6 hours of NAC treatment. Importantly ROS inhibition senitised primary human LEC to necrosis and not apoptosis (data not shown).

Reduced Expression of LC3B in LEC is associated with liver IRI *in vivo*

Our *in vitro* data suggests that ROS-ATG7-mitophagy is an important mechanism for human LEC survival during IRI. We utilised a murine model of partial murine liver IRI to investigate this relationship *in vivo*. As Figure 8 demonstrates partial liver IRI increases serum ALT and AST levels relative to sham-operated mice and H&E liver sections demonstrate that the ischaemic injury in IRI liver lobes was observed within the peri-venular region of the liver with sparing of the peri-portal areas. In accordance with the *in vitro* data, sham operated mice and non-ischaemic/non-IRI liver lobes demonstrated sinusoidal staining with the specific autophagy marker LC3B (Fig 8(ii). This sinusoidal staining was also evident when murine liver tissue from sham-operated mice and was similar to the immunostaining seen with the specific LEC marker CD31. In the IRI liver lobes we observed that both LC3B and CD31 staining is significantly reduced following injury (Fig 8(vi). Using dual immunofluorescence we demonstrate that LC3B colocalises with CD31 in non-injured and sham-operated livers (Fig 8(iii). Following IRI the peri-venular liver sinusoids demonstrated no LC3B or CD31 staining but do demonstrate TUNEL positive cells in the sinusoids (Fig 8(vii) confirming the onset of apoptosis. Furthermore similar to our observations *in vitro* we observed that in non-injured livers ATG7 activity was present with active autophagic flux that is significantly reduced following liver IRI (Fig 8(iv & viii). Taken together this observation support the observation that ATG7-mediated autophagy activation is associated with LEC survival during liver IRI.

Discussion

Liver IRI remains a significant clinical problem following liver transplantation and with the injury targeting the liver parenchymal cells. LEC are the first cell type in the liver to be injured by IRI (5,20,21). ROS generation is a key regulator of liver IRI and was until recently viewed as the primary driver for parenchymal cell death during IRI (22) but more recent studies demonstrate that ROS is cytoprotective through its activation of the cellular process of autophagy (8). Indeed autophagy activation has been shown to limit injury following a variety of acute liver injuries (23-25) and its role in regulating liver IRI is attracting growing attention (11). Limited studies have explored the role of ROS-dependent autophagy during IRI (26,27) but the relationship between ROS and autophagy in LEC during IRI is not known.

Whilst the generation of low amounts of ROS is essential for normal cellular function excess production of ROS is thought to cause cell death (28). The classical cellular response to IRI is an increase in ROS generation during hypoxia that is further accentuated during reperfusion (6). Importantly our *in vitro* model of liver IRI involves the manipulation of oxygen tension and does not recapitulate the other features of IRI such as glucose deprivation. Previous work from our group has shown that intracellular ROS generated in primary human hepatocytes activates autophagy to promote cell survival during IRI (8). We now demonstrate that primary human LEC do not demonstrate this classical response to IRI (18) as they exhibit high levels of intracellular ROS levels that remain unaltered during *in vitro* IRI. Moreover ROS does not induce cell death during IRI but instead is linked to ATG7 activity that can then regulate the downstream autophagy machinery as demonstrated by the formation of LC3B positive puncta and protein analysis consistent with autophagic flux (29). Although ROS-dependent ATG7 activation of autophagy has been reported in other endothelial cell types (30-34) this is the first study to demonstrate this function of autophagy in primary human LEC. Importantly in vascular endothelial cells the ROS-autophagy signalling pathway induces endothelial damage (35) highlighting that autophagy may function differently in cells of different endothelial lineage. Interestingly even in normoxic conditions autophagic puncta are present within primary human LEC that maybe a reflection of the inherent scavenging function that LEC perform within the liver. The critical role of ROS-dependent autophagy activation in LEC is demonstrated by the inhibition of ROS in primary human LEC sensitising cells to necrosis. This data is further corroborated by the selective knockdown of ATG7 also sensitising LEC to necrosis. Importantly our study used DCF to study ROS generation that specifically detects H_2O_2 and the role of other ROS sub-species such as mitochondrial ROS, superoxide (O_2^-) and hydroxyl radicals (OH^-) in regulating LEC autophagy remains to be determined (36). It is important recognise that whilst our *in vitro* model recapitulates many of the features of IRI it does not include the restoration of flow during reperfusion and in particular omits the shear stress and biomechanical alterations that are integral to *in vivo* IRI. These factors may significantly change the autophagic response in LEC during IRI.

The *in vitro* data in the presented in this study suggests that autophagy in primary human LEC involves the selective elimination of dysfunctional mitochondria through the process of mitophagy. Recent studies have demonstrated that specific mitochondrial receptors such a FUNDC1 regulate mitophagy during hypoxia and ensure the timely elimination of dysfunctional mitochondria prior to mitochondrial depolarization (37) and cell death (38) as seen in other acute liver injuries (39). Taken together our study suggests that ROS-dependent mitophagy activation promotes LEC survival. However ROS may also promote LEC survival through activation of autophagy-independent pathways (40,41). In addition autophagy activation in other liver cells may also play a regulatory role during IRI (8) and the relationship between LEC autophagy and these other cells remains to be

determined. Moreover inflammatory signals such as soluble TNFα and cell bound ligands upon inflammatory cells, that are an integral feature of liver IRI (4), may alter LEC autophagy and impact upon LSEC survival. Finally whilst our isolation technique isolates LEC from liver tissue the technique may also harvest vascular endothelium cells as well as liver sinusoidal endothelial cells and thus our cells represent a heterogeneous population of liver endothelial cells.

Our *in vitro* data strongly suggests that autophagy/mitophagy regulates LEC survival during IRI and to assess this mechanism *in vivo* we utilised a murine model of partial liver IRI. Immunohistochemical analysis of murine livers demonstrated that LC3B positive staining was seen in liver sinusoids within uninjured liver lobes, which corresponded to the LEC marker CD31. Dual immunofluorescence confirmed that CD31 and LC3B co-localise within normal liver. Following IRI there is centrilobular necrosis with loss of both LC3B and CD31 immunostaining with concomitant impairment of autophagic flux as demonstrated with Western blotting showing the loss of LC3B and accumulation of p62. Recent studies have suggested that autophagy in LEC is regulated by KLF2 through a Rac1-rab7 pathway (12). These studies suggest that failure to reactivate autophagy during reperfusion by activating KLF2 may regulate the increased cell death in LEC and is associated microvascular dysfunction (12). It remains to be determined whether KLF2 activation is ROS-dependent in LEC or whether alternative signalling pathway such as TFEB (42), AMPK (43), HIF1 (44) and FOXO (45) can also regulate LEC autophagy. Overall our findings suggest that the early injury to LEC during IRI is linked to a disruption in the autophagy-signalling pathway (25,46).

Our finding that NAC causes autophagy inhibition and leads to LEC necrosis during IRI has important clinical implications. It suggests that general antioxidants targeted to the liver may not be an effective intervention to reduce IRI because whilst it may aid hepatocyte survival (6) it will induce LEC death and potentially exacerbate the pro-inflammatory liver microenvironment (47).

In summary our study demonstrates that in primary human LEC ROS-ATG7-dependent autophagy/mitophagy promotes LEC survival during liver IRI suggesting that targeting this signaling pathway in LEC during liver IRI maybe an effective therapeutic strategy to reduce liver injury following surgery.

Acknowledgements

The authors would like to thank the Hepato-pancreatico-biliary/liver transplant surgery team at Queen Elizabeth Hospital, Birmingham, United Kingdom for the access to human liver tissue. Ricky Bhogal was funded by research grant from The Wellcome Trust (DDDP.RCHX14183), St John's Ambulance Travelling Fellowship in Transplantation and Academy of Medical Sciences (DKAA.RCZV18746). The authors would like to thank the National Institute for Health Research Biomedical Research Unit (BRU-2011-20030) for their financial and infrastructure support. The authors are thankful to Michel Weij for expertise in animal surgical techniques.

References

1. Younossi ZM, Koenig AB, Abdelatif D, Fazel Y, Henry L, Wymer M. Global epidemiology of nonalcoholic fatty liver disease-Meta-analytic assessment of prevalence, incidence, and outcomes. Hepatology. 2016;64(1):73-84. doi: 10.1002/hep.28431.

2. Quesnelle KM, Bystrom PV, Toledo-Pereyra LH. Molecular responses to ischemia and reperfusion in the liver. Arch Toxicol. 2015; 89(5):651-7.

3. Cannistrà M, Ruggiero M, Zullo A, Gallelli G, Serafini S, Maria M, Naso A, Grande R, Serra R, Nardo B. Hepatic ischemia reperfusion injury: A systematic review of literature and the role of current drugs and biomarkers. Int J Surg. 2016; Suppl 1:S57-70. doi: 10.1016/j.ijsu.2016.05.050.

4. Zhai Y, Petrowsky H, Hong JC, Busuttil RW, Kupiec-Weglinski JW. Ischaemia–reperfusion injury in liver transplantation—from bench to bedside. Nat Rev Gastroenterol Hepatol. 2013;10(2): 79–89. doi: 10.1038/nrgastro.2012.225

5. Peralta C, Jiménez-Castro MB, Gracia-Sancho J. Hepatic ischemia and reperfusion injury: effects on the liver sinusoidal milieu. J Hepatol. 2013 59(5):1094-106. doi: 10.1016/j.jhep.2013.06.017.

6. Bhogal RH, Curbishley SM, Weston CJ, Adams DH, Afford SC. Reactive oxygen species mediate human hepatocyte injury during hypoxia/reoxygenation. Liver Transpl. 2010; 16(11):1303-13. doi: 10.1002/lt.22157.

7. Shibuya H, Ohkohchi N, Seya K, Satomi S. Kupffer cells generate superoxide anions and modulate lipid peroxidation and mitochondrial proton ATP-ASE activity in the perfused rat liver after cold preservation. Transplant Proc. 1997 29(1-2):1328-30.

8. Bhogal RH, Weston CJ, Curbishley SM, Adams DH, Afford SC. Autophagy: A cyto-protective mechanism which prevents primary human hepatocyte apoptosis during oxidative stress. Autophagy. 2012;1;8(4). doi: 10.4161/auto.19012

9. Cursio R, Colosetti P, Gugenheim J. Autophagy and liver ischemia-reperfusion injury. Biomed Res Int. 2015;2015:417590.

10. NN Noda, F Inagaki F. Mechanisms of autophagy. Annu Rev Biophys. 2015;44: 101-122

11. KL Go, S Lee, I Zendejas, KE Behrns, JS Kim. Mitochondrial Dysfunction and Autophagy in Hepatic Ischemia/Reperfusion Injury. Biomed Res Int 2015;2015: 183469

12. Guixé-Muntet S, de Mesquita FC, Vila S, Hernández-Gea V, Peralta C, García-Pagán JC, Bosch J, Gracia-Sancho J. Cross-talk between autophagy and KLF2 determines endothelial cell phenotype and microvascular function in acute liver injury. J Hepatol. 2017;66(1):86-94. doi: 10.1016/j.jhep.2016.07.051.

13. Wang K. Autophagy and apoptosis in liver injury. Cell Cycle. 2015;14(11):1631-42. doi: 10.1080/15384101.2015.1038685

14. Zeng M, Wei X, Wu Z, Li W, Li B, Fei Y, He Y, Chen J, Wang P, Liu X. Reactive oxygen species contribute to simulated ischemia/reperfusion-induced autophagic cell death in human umbilical vein endothelial cells. Med Sci Monit. 2014;20:1017-23.

15. Shiroto T, Romero N, Sugiyama T, Sartoretto JL, Kalwa H, Yan Z, Shimokawa H, Michel T. Caveolin-1 is a critical determinant of autophagy, metabolic switching, and oxidative stress in vascular endothelium. PLoS One. 2014;9(2):e87871.

16. Lalor PF, Edwards S, McNab G, Salmi M, Jalkanen S, Adams DH. Vascular adhesion protein-1 mediates adhesion and transmigration of lymphocytes on human hepatic endothelial cells. J Immunol. 2002;169(2):983-92.

17. Lalor PF, Lai WK, Curbishley SM, Shetty, Adamd DH. Human hepatic sinusoidal endothelials cells can be distinguised by expression of phenotypic markers related to their specialised functions in vivo. World J Gastroenterol. 2006; 12(34): 5429-39

18. Laing RW, Bhogal RH, Wallace L, Boteon Y, Neil DAH, Smith A, Stephenson BTF, Schlegel A, Hübscher SG, Mirza DF et al. THE USE OF AN ACELLULAR OXYGEN CARRIER IN A HUMAN LIVER MODEL OF NORMOTHERMIC MACHINE PERFUSION. Transplantation. 2017;doi: 10.1097/TP.0000000000001821.

19. Chen Z, Siraj S, Liu L, Chen Q. MARCH5-FUNDC1 axis fine-tunes hypoxia-induced mitophagy. Autophagy. 2017;13(7):1244-1245. doi: 10.1080/15548627.2017.1310789

20. Gracia-Sancho J, Casillas-Ramirez A, Peralta C. Molecular pathways in protecting the liver from ischaemia/reperfusion injury: a 2015 update. Clin Sci (Lond). 2015;129(4):345-62.

21. Kohli V, Selzner M, Madden JF, Bentley RC, Clavien PA. Endothelial cell and hepatocyte deaths occur by apoptosis after ischemia-reperfusion injury in the rat liver. Transplantation. 1999;67(8):1099-105

22. Samarasinghe DA, Farrell GC. The central role of sinusoidal endothelial cells in hepatic hypoxia-reoxygenation injury in the rat. Hepatology. 1996;24(5):1230-7.

23. Peixoto E, Atorrasagasti C, Aquino JB, Militello R, Bayo J, Fiore E, Piccioni F, Salvatierra E, Alaniz L, García MG et al. SPARC (secreted protein acidic and rich in cysteine) knockdown protects mice from acute liver injury by reducing vascular endothelial cell damage. Gene Ther. 2015; 22(1):9-19. doi: 10.1038/gt.2014.102.

24. Zhong C, Pu LY, Fang MM, Gu Z, Rao JH, Wang XH. Retinoic acid receptor α promotes autophagy to alleviate liver ischemia and reperfusion injury. World J Gastroenterol. 2015;21(43):12381-91. doi: 10.3748/wjg.v21.i43.12381.

25. Esposti DD, Domart MC, Sebagh M, Harper F, Pierron G, Brenner C, Lemoine A. Autophagy is induced by ischemic preconditioning in human livers formerly treated by chemotherapy to limit necrosis. Autophagy. 2010;6(1):172-4.

26. Gracia-Sancho J, Guixe-Muntet S, Hide D, Bosch J. Modulation of autophagy for the treatment of liver diseases. Expert Opin Investig Drugs 2014;23(7): 965-977

27. Rautou PE, Mansouri A, Lebrec D, Durand F, Valla D, Moreau R. Autophagy in liver diseases. J Hepatol. 2010;53(6):1123-34. doi: 10.1016/j.jhep.2010.07.006.

28. Vakifahmetoglu-Norberg H, Ouchida AT, Norberg E. The role of mitochondria in metabolism and cell death. Biochem Biophys Res Commun. 2017 Jan 15;482(3):426-431. doi: 10.1016/j.bbrc.2016.11.088.

29. Chen Y, Azad MB, Gibson SB. Superoxide is the major reactive oxygen species regulating autophagy. Cell Death Differ. 2009;16(7):1040-52. doi: 10.1038/cdd.2009.49.

30. Han J, Pan XY, Xu Y, Xiao Y, An Y, Tie L, Pan Y, Li XJ. Curcumin induces autophagy to protect vascular endothelial cell survival from oxidative stress damage.

Autophagy. 2012;8(5):812-25. doi: 10.4161/auto.19471.

31. Shen W, Tian C, Chen H, Yang Y, Zhu D, Gao P, Liu J. Oxidative stress mediates chemerin-induced autophagy in endothelial cells. Free Radic Biol Med. 2013;55:73-82. doi: 10.1016/j.freeradbiomed.2012.11.011.

32. Liu J, Bi X, Chen T, Zhang Q, Wang SX, Chiu JJ, Liu GS, Zhang Y, Bu P, Jiang F. Shear stress regulates endothelial cell autophagy via redox regulation and Sirt1 expression. Cell Death Dis. 2015;16;6:e1827. doi: 10.1038/cddis.2015.193.

33. Tang ZH, Cao WX, Wang ZY, Lu JH, Liu B, Chen X, Lu JJ. Induction of reactive oxygen species-stimulated distinctive autophagy by chelerythrine in non-small cell lung cancer cells. Redox Biol. 2017 Aug;12:367-376. doi: 10.1016/j.redox.2017.03.009.

34. Teng RJ, Du J, Welak S, Guan T, Eis A, Shi Y, Konduri GG. Cross talk between NADPH oxidase and autophagy in pulmonary artery endothelial cells with intrauterine persistent pulmonary hypertension. Am J Physiol Lung Cell Mol Physiol. 2012;302(7):L651-63. doi: 10.1152/ajplung.00177.2011.

35. Tang X, Lin C, Guo D, Qian R, Li X, Shi Z, Liu J, Li X, Fan L. CLOCK Promotes Endothelial Damage by Inducing Autophagy through Reactive Oxygen Species. Oxid Med Cell Longev. 2016;2016:9591482. doi: 10.1155/2016/9591482.

36. Schieber M, Chandel NS. ROS function in redox signaling and oxidative stress. Curr Biol. 2014 May 19;24(10):R453-62. doi: 10.1016/j.cub.2014.03.034.

37. Chen Z, Liu L, Cheng Q, Li Y, Wu H, Zhang W, Wang Y, Sehgal SA, Siraj S, Wang X et al. Mitochondrial E3 ligase MARCH5 regulates FUNDC1 to fine-tune hypoxic mitophagy. EMBO Rep. 2017 Mar;18(3):495-509. doi: 10.15252/embr.201643309.

38. Hu C, Li L. Pre-conditions for eliminating mitochondrial dysfunction and maintaining liver function after hepatic ischaemia reperfusion. J Cell Mol Med. 2017;21(9):1719-1731. doi: 10.1111/jcmm.13129.

39. Gao Y, Chu S, Zhang Z, Zuo W, Xia C, Ai Q, Luo P, Cao P, Chen N. Early Stage Functions of Mitochondrial Autophagy and Oxidative Stress in Acetaminophen-Induced Liver Injury. J Cell Biochem. 2017;118(10):3130-3141. doi: 10.1002/jcb.25788.

40. Al-Mehdi AB, Pastukh VM, Swiger BM, Reed DJ, Patel MR, Bardwell GC, Pastukh VV, Alexeyev MF, Gillespie MN. Perinuclear mitochondrial clustering creates an oxidant-rich nuclear domain required for hypoxia-induced transcription. Sci Signal. 2012;5(231):ra47. doi: 10.1126/scisignal.2002712.

41. Connor KM, Subbaram S, Regan KJ, Nelson KK, Mazurkiewicz JE, Bartholomew PJ, Aplin AE, Tai YT, Aguirre-Ghiso J, Flores SC et al. Mitochondrial H2O2 regulates the angiogenic phenotype via PTEN oxidation. J Biol Chem. 2005;280(17):16916-24.

42. Neill T, Sharpe C, Owens RT, Iozzo RV. Decorin-Evoked Paternally Expressed Gene 3 (PEG3) is an Upstream Regulator of the Transcription Factor EB (TFEB) in Endothelial Cell Autophagy. Redox Biol. 2017 Oct;13:508-521. doi: 10.1016/j.redox.2017.07.011

43. Luo X, Dan Wang, Luo X, Zhu X, Wang G, Ning Z, Li Y, Ma X, Yang R, Jin S et al. Caveolin 1-related autophagy initiated by aldosterone-induced oxidation promotes liver sinusoidal endothelial cells defenestration. Biomed Pharmacother. 2017;93:885-894. doi: 10.1016/j.biopha.2017.07.044

44. Anavi S, Hahn-Obercyger M, Madar Z, Tirosh O. Mechanism for HIF-1 activation by cholesterol under normoxia: a redox signaling pathway for liver damage. J Cell Mol Med. 2017 Sep;21(9):1719-1731. doi: 10.1111/jcmm.13129.

45. Boteon Y, Laing R, Mirza DF, Mergental H, Bhogal RH. The regulation of endothelial cell autophagy and its targeting during normothermic machine liver perfusion. World J Gastro 2017; In press DOI: 10.3748

46. Yang MC, Chang CP, Lei HY. Endothelial cells are damaged by autophagic induction before hepatocytes in Con A-induced acute hepatitis. Int Immunol. 2010 Aug;22(8):661-70. doi: 10.1093/intimm/dxq050.

47. Shi S, Xue F. Current Antioxidant Treatments in Organ Transplantation. Oxid Med Cell Longev. 2016;2016:8678510. doi: 10.1155/2016/8678510.

Figure Legends

Figure 1. Intracellular ROS Levels in Primary Human LEC during *in vitro* IRI

(i) Demonstrates a typical forward scatter (FS) versus side scatter (SS) plot of primary human LEC. The FS versus SS plots shown is from the hypoxia sample of a liver preparation but similar plots were obtained during normoxia and hypoxia (data not shown).

(ii) Illustrates a representative flow cytometry plot of intracellular ROS content in primary human LEC during normoxia (black), hypoxia (red) and H-R (blue). The experiment was repeated at least 7 times in doublet. Data are expressed as MFI and readings are based upon values taken from cells within the gated region in Fig 1(i).

(iii) The bar chart represents pooled data of at least 7 separate experiments illustrating intracellular ROS content in primary LEC during normoxia, hypoxia and H-R. Data are expressed as MFI and readings are based upon values taken from cells within the gated region in Fig 1(i).

Figure 2. N-Acetylcysteine Induces a Time-Dependent Decrease in Intracellular ROS in Primary Human LEC during *in vitro* IRI

Isolated primary human LEC were exposed to normoxia, hypoxia or H-R in the presence or absence of the general antioxidant NAC. Representative flow cytometry plots illustrate the effect of NAC on primary human LEC intracellular ROS content during normoxia, hypoxia and H-R. FS versus SS plots of primary human LEC are the same as those illustrated in Fig 1(i) (data not shown). The bar chart adjacent to the plots demonstrates the pooled data of four separate experiments illustrating the effects of NAC upon human LEC ROS content during each of the three experimental conditions. Data is expressed as MFI and readings are based upon values taken from cells within the gated region shown in Fig 1(i). Data are expressed as mean ± S.E. (*$p<0.05$).

Figure 3. Intracellular ROS in Primary Human LEC Regulates ATG7 Activity and Autophagic Flux during *in vitro* IRI

(i) Following normoxia, hypoxia and H-R primary human LEC were lysed and expression of ATG7, LC3B and p62 was assessed by Western blotting as described in the Methods and Materials section. LEC were incubated with NAC for the stated times in the either normoxia, hypoxia or H-R. All western blots were performed at least three times and presented blots are representative of all samples (n=3). (ii) Blots were then analysed using denisometric analysis and values normalized to β-actin loading controls (n=3). Data are expressed as mean ± S.E. (*$p<0.05$, **$p<0.01$, ***$p<0.001$).

Figure 4. siRNA ATG7 Knockdown in Human LEC does not Affect Intracellular ROS Production but does Alter Autophagic Flux and Sensitises Human LEC to Necrosis

(i) Lipofectamine based transfection of primary human LEC with ATG7 siRNA led to a 60% knockdown in expression as verified by PCR expression of ATG7 mRNA. (ii) Following 24 hours of

normoxia, hypoxia and H-R primary human LEC were lysed and expression of ATG7, LC3B and p62 was assessed by Western blotting as described in the Methods and Materials section. All western blots were performed at least three times and presented blots are representative of all samples (n=3). Blots were then analysed using denisometric analysis and values normalized to β actin loading controls (n=3), Data are expressed as mean ± S.E. (*p<0.05). (iii) Representative flow cytometry plots illustrate the effect of the ATG7 knockdown upon primary human LEC necrosis during *in vitro* IRI. LEC were exposed to 24 hours of normoxia, hypoxia and H-R. Percentage positive cells for the ROS probe DCF are shown on the x-axis and the necrosis marker 7-AAD is shown on the y-axis. The percentage of cells that demonstrate necrosis is shown in parentheses. Experiments were performed at three times in doublet (n=3).

Figure 5. Intracellular ROS Regulates LC3B Positive Puncta in Primary Human LEC during IRI

(i) Primary human LEC were exposed to normoxia, hypoxia and H-R in the absence and absence of NAC. Following the desired incubation period LEC were fixed and permeabilised. LC3B positive puncta within LEC was assessed using immunofluorescence and representative images are shown (n=3). (ii) LC3B positive puncta in LEC were quantified using image analysis. NAC significantly reduces LC3B positive puncta in primary human LEC during normoxia, hypoxia and H-R. Data are expressed as mean ± S.E. (*p<0.01) (n=3).

Figure 6. LC3B and TOMM20 Co-localise in Primary Human LEC during IRI

(i) Primary human LEC were exposed to normoxia, hypoxia and H-R for 6 hours in the presence and absence of NAC. Cells were fixed and permeabilized and LEC expression for LC3B (red) and TOMM20 (green) assessed using immunofluorescence. DAPI was used for nuclear staining and composite overlay images are shown on the right. Experiments were performed at least three times and representative images are shown (n=3).

(ii) LC3B positive puncta and TOMM20 staining in LEC were quantified using image analysis. NAC significantly reduces dual LC3B/TOMM20 positive puncta in primary human LEC during normoxia, hypoxia and H-R, Data are expressed as mean ± S.E. (*p<0.01) (n=3).

Figure 7. Intracellular ROS Inhibition with N-acetylcysteine Increases Primary Human LEC Necrosis during *in vitro* IRI

Representative flow cytometry plots illustrate the effect of the NAC upon primary human LEC necrosis during *in vitro* IRI in the presence and absence of NAC. Percentage positive cells for the ROS probe DCF are shown on the x-axis and the necrosis marker 7-AAD is shown on the y-axis. The percentage of cells that demonstrate necrosis is shown in parentheses. Experiments were performed at three times in doublet (n=3).

Figure 8. Reduced Expression of LC3B in LEC is associated with Liver IRI in vivo

(i) Demonstrates serum AST/ALT levels in C57/B6 mice following sham operations and exposure to liver IRI (n=9-10). (ii) The top panel demonstrates the increased liver injury seen in the liver following IRI as assessed by H&E staining. The middle panel demonstrates CD31 immunostaining in sham, non-IRI and IRI of the liver and the bottom panel demonstrates the pattern of staining with the specific autophagy marker LC3B (n=5-7). (iii) demonstrates the percentage area stained by LC3B and CD31 in murine liver sections following sham operations, non-injured lobes and liver IRI. Data are expressed as mean ± S.E. (*$p<0.05$) (n=5-7). (iv) FFPE murine liver tissue was assess for LC3B (red) and CD31 (green) expression in sham, non-IRI and IRI liver lobes. Overlay images are also demonstrated. TUNEL stained murine liver tissue is demonstrated on the right with apoptotic cells within the liver sinusoids shown with the white asterisks (n=5-7). (v) Whole murine liver lysates were assessed for ATG7, LC3B and p62 expression and representative blots are shown. All western blots were performed at least three times (n = 3). (vi) demonstrates the relative intensity of LC3B and CD31 immunofluoresence for the data presented in Fig 8(iv) (n=5-7). Data are expressed as mean ± S.E. (*$p<0.05$). (vii) Demonstrates the number of TUNEL positive LEC in liver sections following sham-operations, non-injured liver lobes and liver IRI lobes (n=5-7). Data are expressed as mean ± S.E. (*$p<0.05$). (viii) Shows denisometric analysis of whole liver lysates analysed for LC3B, ATG7 and p62. Values have been normalized to β-actin loading controls (n=3). Data are expressed as mean ± S.E. (*$p<0.05$).

Figure 1. Primary Human LEC Demonstrate High Intracellular ROS Levels during in vitro IRI

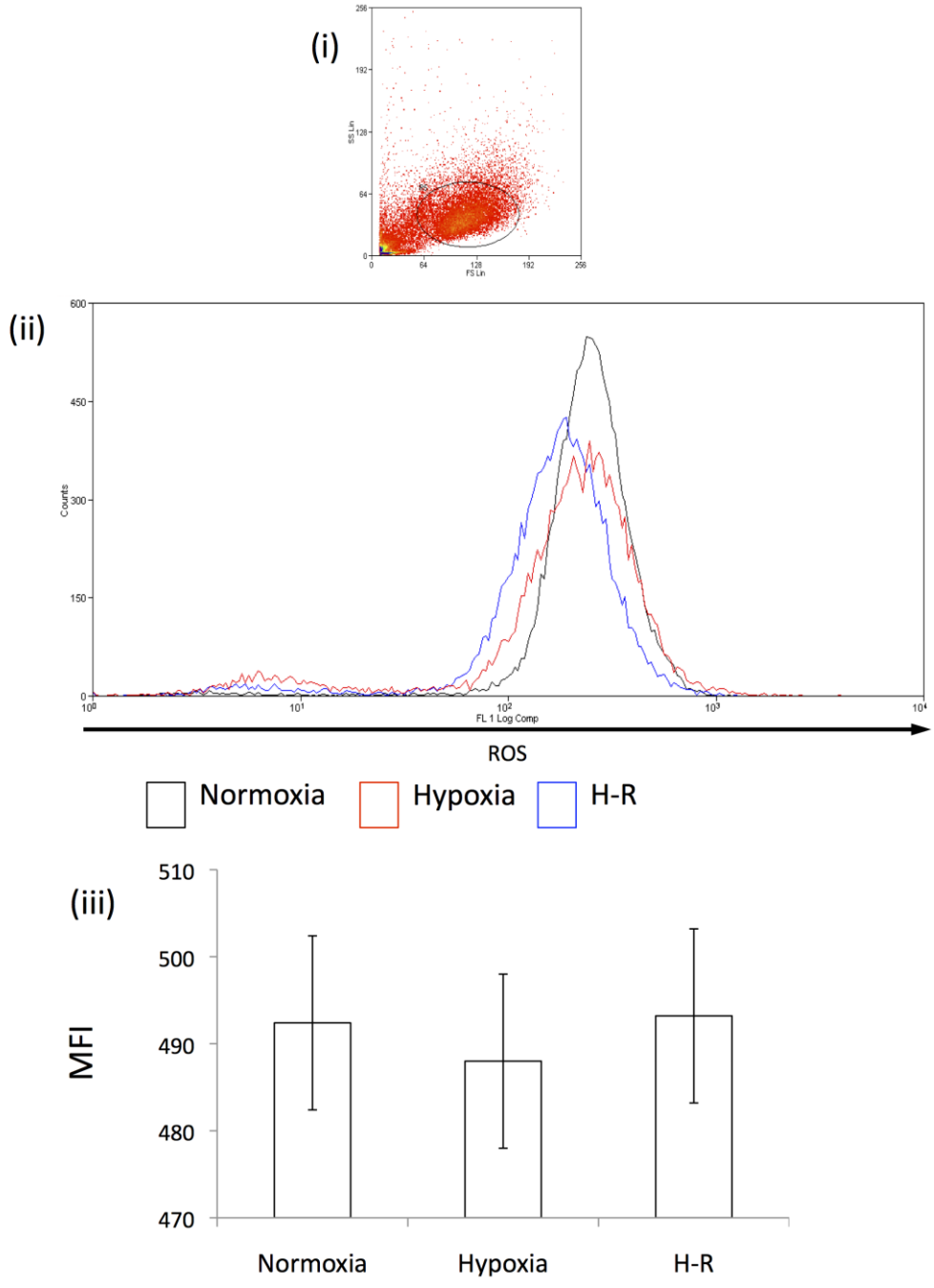

Figure 2. N-acetylcysteine Induces a Time-Dependent Decrease in Intracellular ROS in Primary Human LEC during in vitro IRI

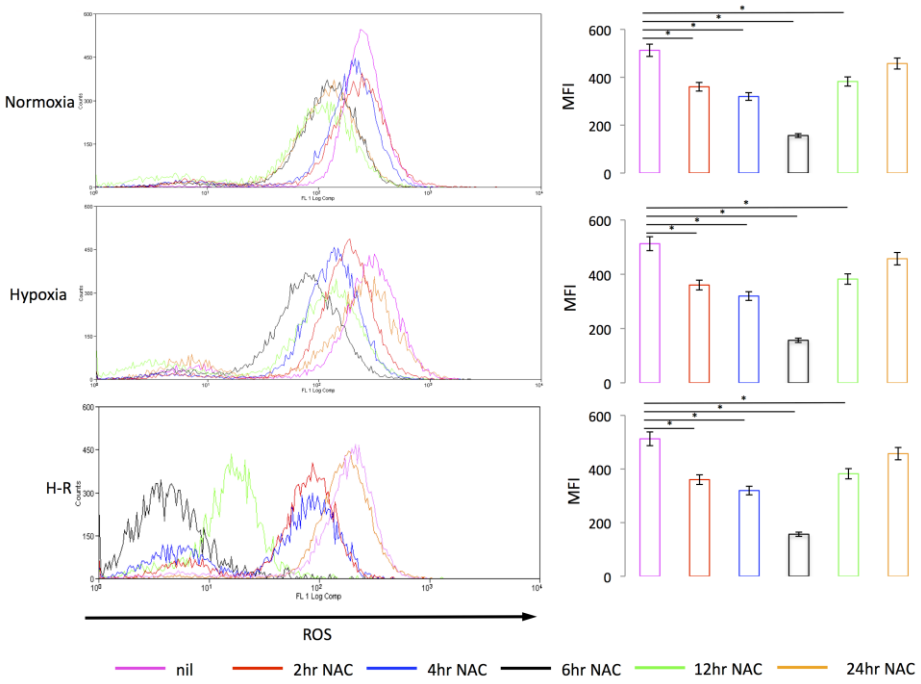

Figure 3. Intracellular ROS in Primary Human LEC Regulates ATG7 Activity and Autophagic Flux during *in vitro* IRI

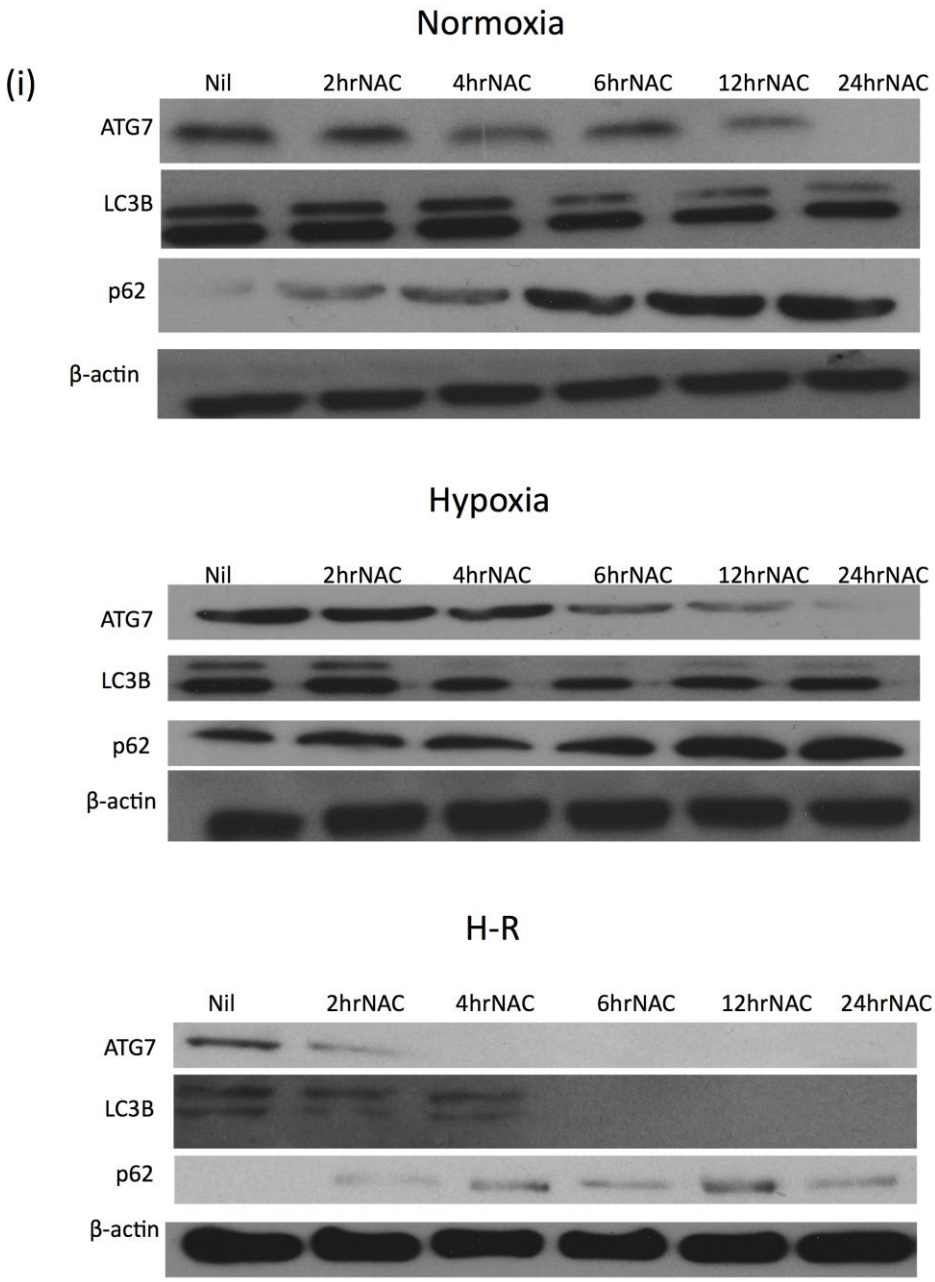

Figure 4. siRNA ATG7 Knockdown in Human LEC does not Affect Intracellular ROS Production but does Alter Autophagic Flux and Sensitises Human LEC to Necrosis

(i)

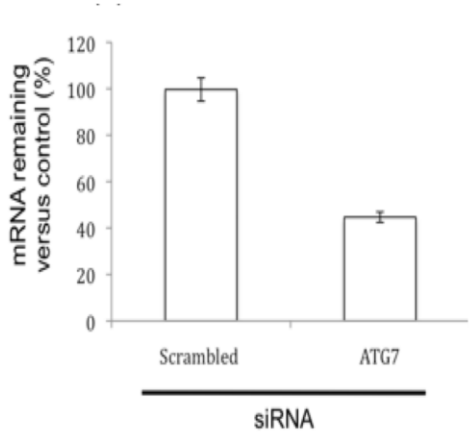

Figure 5: Intracellular ROS Regulates LC3B Puncta in Human LEC during IRI

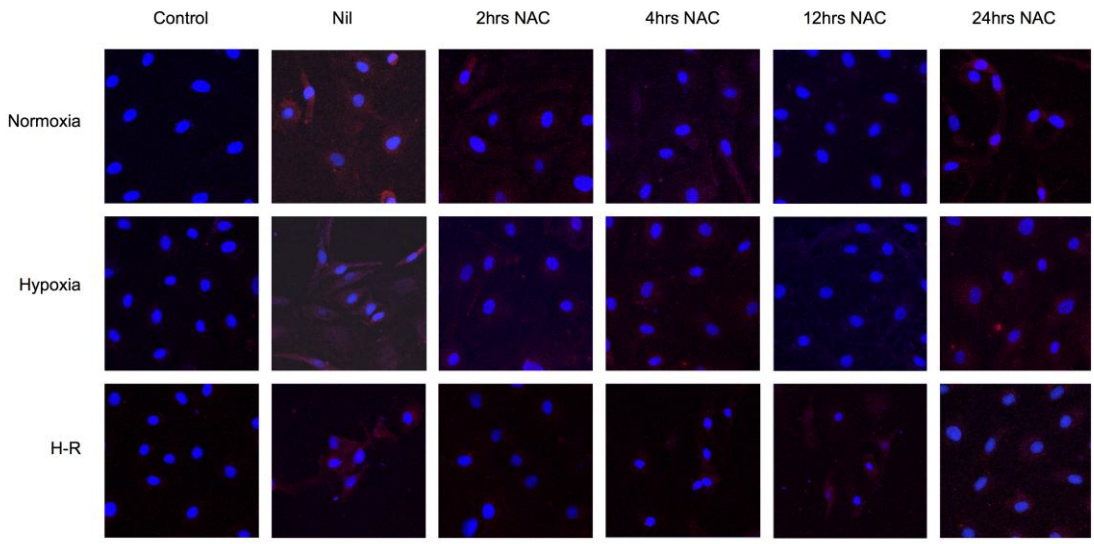

(ii)

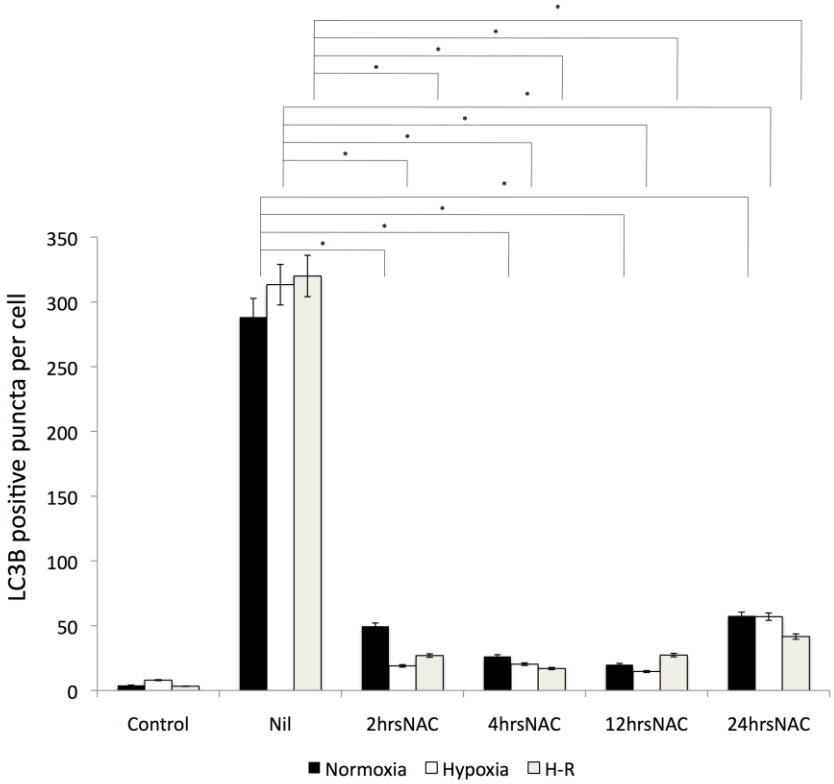

Figure 6. LC3B and TOMM20 Co-localise in Primary Human LEC during IRI

(i)

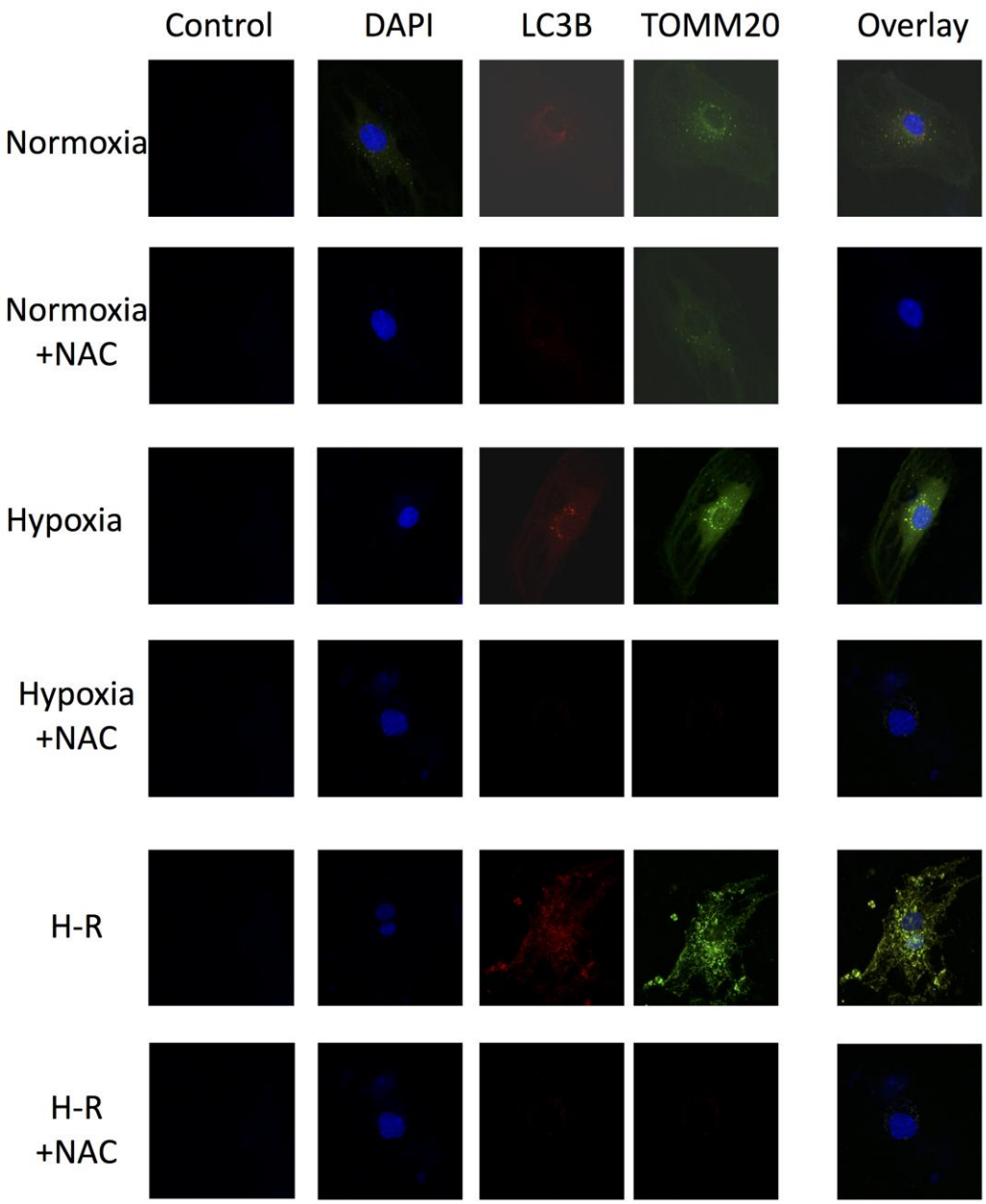

Figure 6: LC3B and TOMM20 Co-localise in Primary Human LEC during IRI

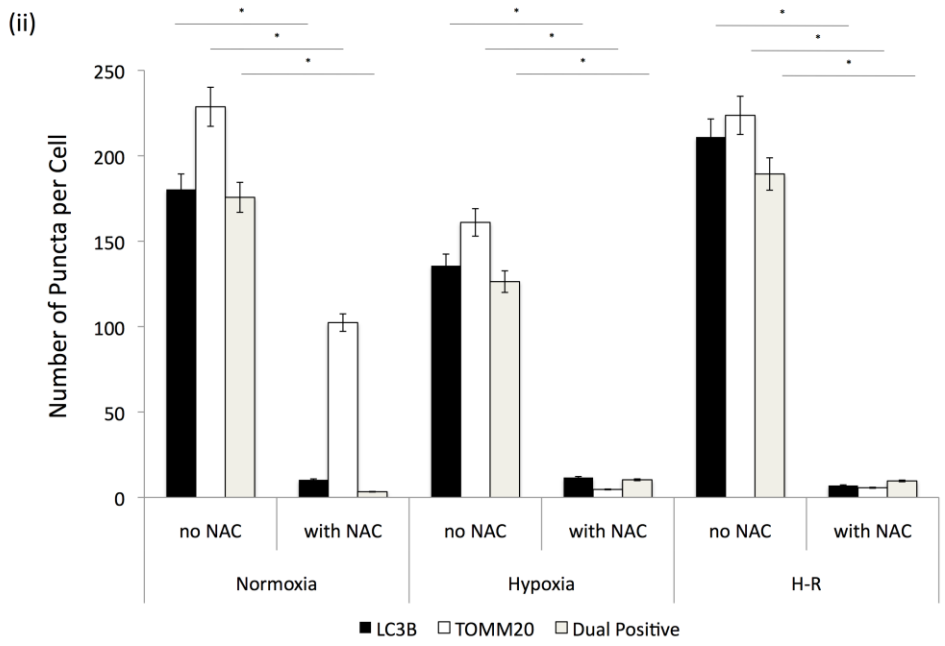

Figure 7. Intracellular ROS Inhibition with N-acetylcysteine Increases Primary Human LEC Necrosis during in vitro IRI

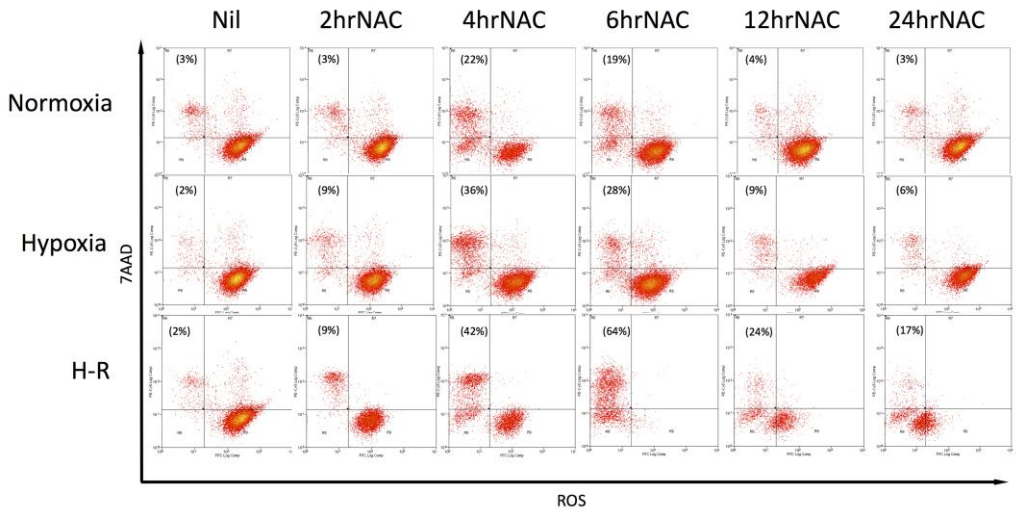

Figure 8. Reduced Expression of LC3B in LEC is associated with Liver IRI in vivo

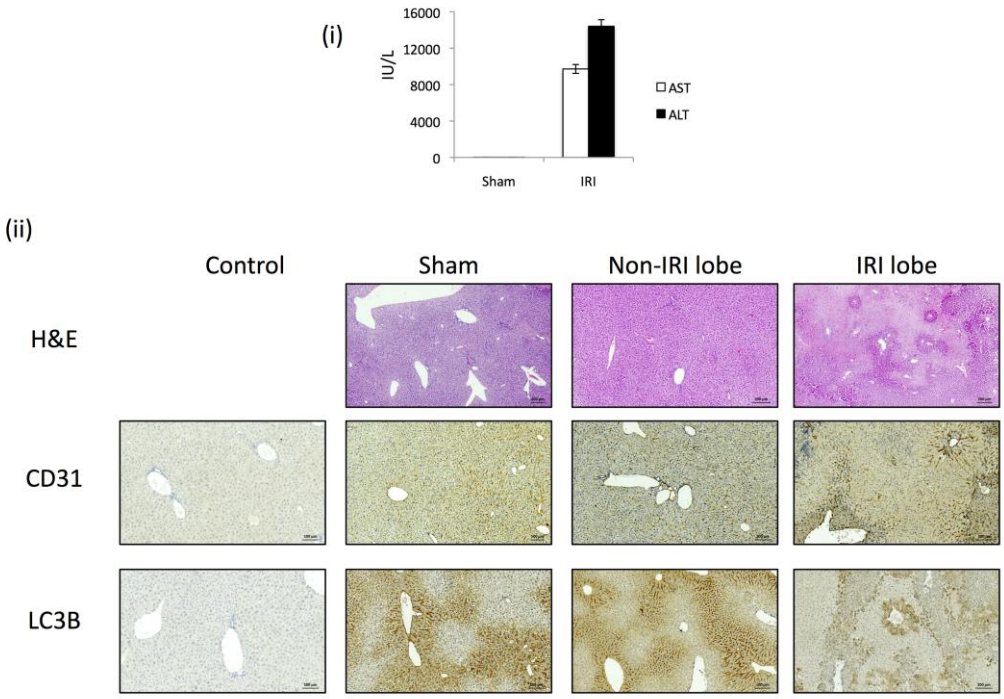

Figure 8. Reduced Expression of LC3B in LEC is associated with Liver IRI in vivo

(iii)

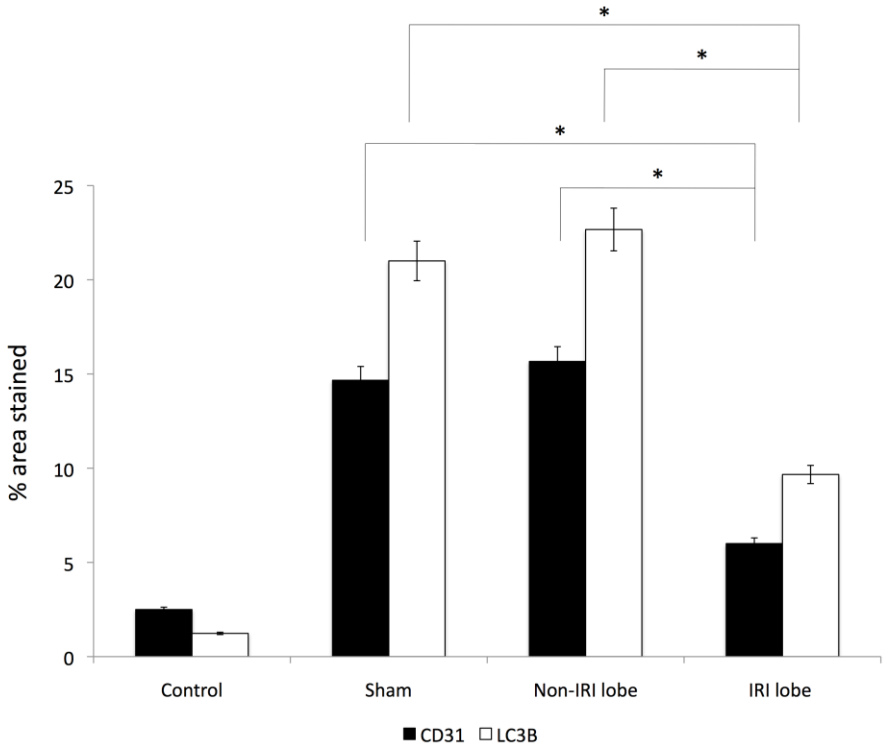

Figure 8. Reduced Expression of LC3B in LEC is associated with Liver IRI in vivo

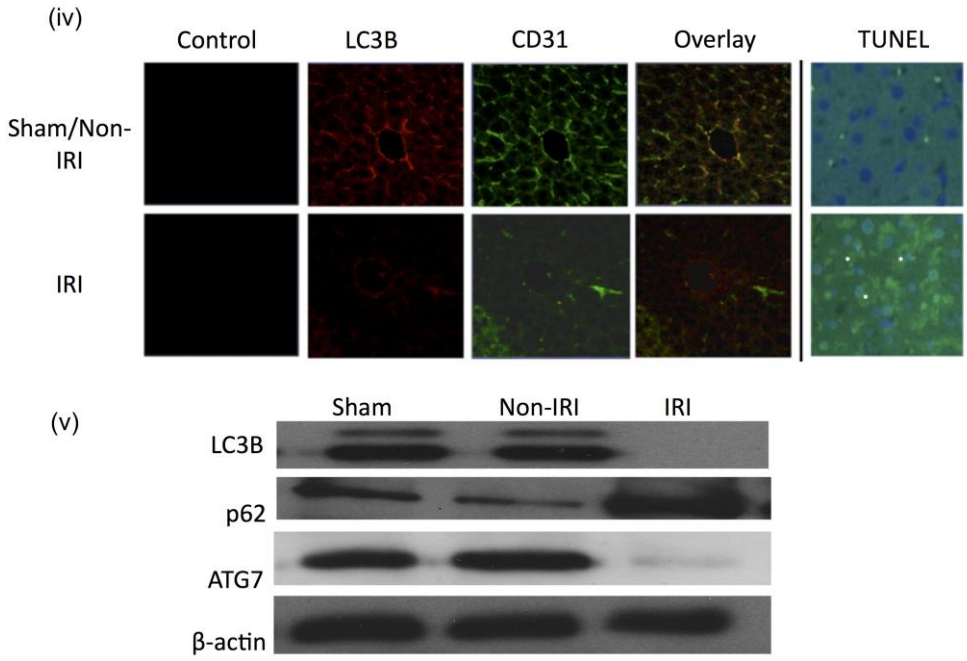

Figure 8. Reduced Expression of LC3B in LEC is associated with Liver IRI in vivo